Proc. Indian Acad. Sci. (Earth Planet. Sci.), Vol. 97, No. 2, December 1988, pp. 117–125.

Cosmic-ray production rates of neon isotopes in meteorite minerals

N. BHANDARI

Keywords. Meteorites; solar flares; galactic cosmic rays; neon isotopes.

1. Introduction

The concentration of ^{21}Ne in stony meteorites provides a reliable method of determining their exposure ages and the ratio $^{22}Ne/^{21}Ne$ is useful in understanding the exposure history of the meteoroid and estimating the atmospheric ablation and shielding depth. Furthermore the three isotopes of neon (20, 21 and 22) provide an accurate method of correcting for any primordial component and identifying grains irradiated by solar flare particles during precompaction stage of the meteoroid. Measurements in mineral separates are sometimes more useful than those in the bulk meteorite because they provide a comparatively clearer picture of the irradiation history of the meteorite. We have therefore calculated the rates of production of ^{21}Ne and ^{22}Ne due to galactic (GCR) and solar (SCR) particles in some common silicate minerals which are abundant in chondrites.

2. Methodology

The isotope production rates due to galactic cosmic rays depend on target element abundances, excitation functions and energy spectra of primary and secondary nucleons which, in turn, depend upon the size of the meteoroid and shielding depth. Here we follow the model of Bhandari and Potdar (1982) for calculating the flux of nucleons as a function of energy at various depths within a meteoroid of a given size. The GCR flux in the interplanetary space of 1·7 P/cm^2. sec. 4π ster. (> 1 BeV) is used here following Reedy and Arnold (1972). This represents a long-term (10^6–10^7 years) average flux at 1 A.U. near the ecliptic. The energy spectra of nucleons within the

meteorite are determined from the spectral shape parameter α, based on the experimental work of Bhattacharya *et al* (1980) and Potdar *et al* (1986) who determined this parameter for spherical meteoroids of radii 6, 9, 15, 25, 50 and >400 cm. Proton and neutron cross-sections for the production of neon isotopes for different target elements at some energies have been measured (Reedy and Arnold 1972 and references therein; Walton 1974; Walton *et al* 1976; Tobailem and Lassus St Genies 1977; Reedy *et al* 1979; Tobailem 1981; Baros and Regnier 1984). Michel *et al* (1986) and Aylmer *et al* (1987) determined some excitation functions from simulated thick target irradiations to proton beams as well as from thin target experiments. The excitation functions used here are the same as those adopted by Bhandari and Potdar (1982). In the case of ^{22}Ne, direct production from various elements as well as via decay of ^{22}Na has been taken into account. There is some uncertainty in the excitation functions because of the lack of measurements, particularly for neutron-induced reactions. In such cases excitation functions for neutron-induced reactions are taken to be the same as those for the analogous proton-induced reactions. This introduces some uncertainty in the production rates but is not serious since the ^{21}Ne and ^{22}Ne/^{21}Ne ratio profiles agree well with the measured values in San Juan Capistrano, St Severin and Keyes meteorites (Bhandari and Potdar 1982). The ^{22}Ne/^{21}Ne profiles also agree with the Berne data (Eberhardt *et al* 1966). However, there is some uncertainty in the estimation of exposure ages of these meteorites. In their work Bhandari and Potdar (1982) used the mean values of the exposure ages—11·2 Ma for St Severin and 19 Ma for San Juan Capistrano and Keyes. New analysis (Graf *et al* 1986) indicates somewhat higher exposure ages. If this is true the production rates given here will have been overestimated by the same factor, although the ^{22}Ne/^{21}Ne ratio would be unaffected. The adopted abundances of Mg, Al, Si and Na, which are the main target elements in silicate minerals, are given in table 1 (Allen and Mason 1973).

A similar procedure is used for calculating the production rates due to solar cosmic rays except that, because of the low energy of primary protons, it is not necessary to consider secondary nucleon production. There is some uncertainty in the estimates of long-term average solar flare proton fluxes. The values of flux $J_s(>10\,\text{MeV/cm}^2$, sec. 4π ster) and rigidity R_0 (MV) have been determined from studies of lunar rocks (Bhandari *et al* 1975; Kohl *et al* 1978). We use here two sets of energy spectra defined by (J_s, R_0) = (i) (125, 125) and (ii) (100, 100). The solar proton flux, however, depends upon the heliocentric distance, being high near the sun, at the meteoroid perihelion, and decreasing significantly with distance as the meteoroid moves towards its aphelion, where it spends most of its time. The average flux, integrated over the orbit, has been found to be as low as (40, 100) for the St Severin meteorite (Lal and Marti 1977; Bhandari and Potdar 1982).

Table 1. Adopted abundances (%) of main target elements in silicate minerals.

	Mg	Al	Si	Na
Olivine	23·9	0·01	17·8	0·02
Feldspar	0·04	11·0	30·5	7·0
Orthopyroxene	17·7	0·06	26·0	0·03
Clinopyroxene	10·1	0·3	25·3	0·43

3. Results and discussion

The production profiles of ^{21}Ne due to GCR and the ^{22}Ne/^{21}Ne ratio in clinopyroxene, olivine, orthopyroxene and feldspar in meteorites of different radii, i.e. 9, 15, 25, 50 cm and infinitely large (> 400 cm), are shown in figure 1(a and b). It can be seen that the isotope production rate first increases with depth, with the development of nuclear cascade reaching a maximum around 10–20 cm depth, and then, in larger meteorites, decreasing with subsequent attenuation of nucleons. Typical GCR production rates of ^{21}Ne from different target elements, i.e. Mg, Al and Si, in a spherical meteoroid of 50 cm radius at a depth of 20 cm within the meteoroid are given in table 2 to show their relative importance. The ^{22}Ne/^{21}Ne ratios are given in table 3.

Calculations show that the GCR production profiles of ^{21}Ne and ^{22}Ne in major target elements follow a similar trend with depth, resulting in a monotonously decreasing ^{22}Ne/^{21}Ne profile in olivines and pyroxenes. The ^{22}Na production from Na, which is produced in (n, $2n$) reaction, has a relatively flat profile compared to its production in other target elements. For this reason, in feldspars which contain large amounts of Na, the (^{22}Ne + ^{22}Na)/^{21} Ne ratio increases with depth. Starting around 1·6 near the surface, the ^{22}Ne/^{21}Ne ratio attains a value of 2·4 at a depth of 50 cm in large meteoroids, mainly owing to this reaction. The neon ratio in feldspars is thus, to a first approximation, sensitive to the pre-atmospheric size of the meteoroid. The isotopes ^{21}Ne and ^{22}Ne are also favourably produced in (n, alpha) reaction on ^{24}Mg and ^{25}Mg respectively. As ^{24}Mg isotopic abundance (78·99%) is much higher than ^{25}Mg abundance (10%) in olivines, where Mg content is high, the ^{22}Ne/^{21}Ne ratio remains low (between 1·2 and 0·98) for large meteoroids. The lowest production of ^{21}Ne occurs in feldspars and the highest in olivines because of the abundance of Mg which is the main target. The ^{22}Ne/^{21}Ne ratio in olivines and pyroxenes decreases from 1·2 or 1·3 near the surface to a value around 1 at a depth of 50 cm in large meteoroids.

Table 2. GCR production rate of ^{21}Ne (10^{-8} cc STP g. Ma) in various minerals for different target elements in a 50 cm radius meteoroid at a depth of 20 cm.

	Mg	Al	Si	Total
Olivine	0·468	0·00	0·078	0·546
Feldspar	0·001	0·06	0·133	0·194
Orthopyroxene	0·347	0·001	0·144	0·462
Clinopyroxene	0·198	0·002	0·111	0·311

Table 3. Spallation ^{22}Ne/^{21}Ne ratio in various target elements in a 50 cm radius meteoroid.

Shielding depth	Mg	Al	Si
3 cm	1·032	1·25	1·32
At centre	0·96	1·33	1·36

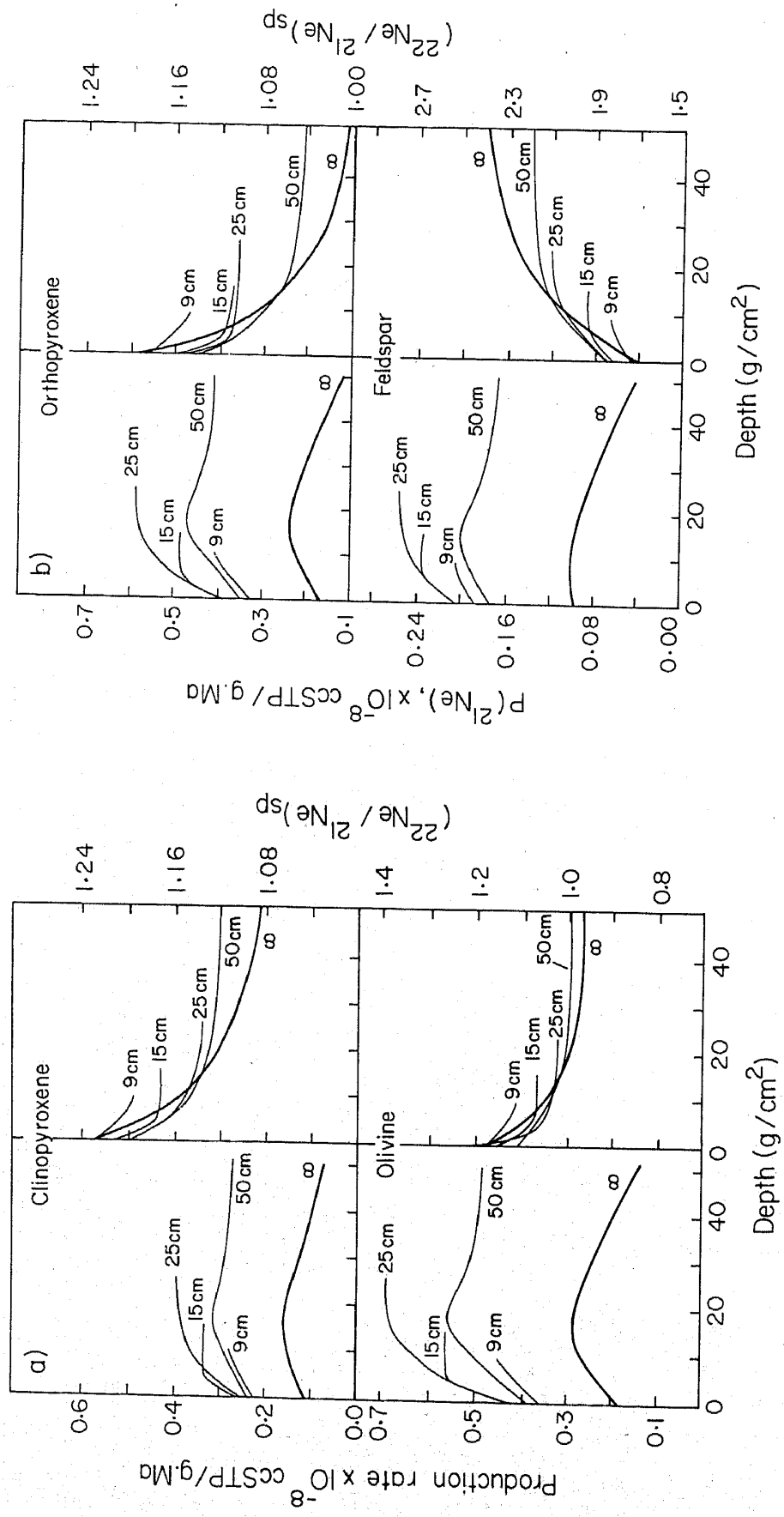

Figure 1. ^{21}Ne production rate (P(^{21}Ne)) due to galactic cosmic rays and (^{22}Ne/^{21}Ne)$_{sp}$ in various minerals as a function of meteoroid radius and depth of sample in (a) clinopyroxene and olivine; (b) orthopyroxene and feldspar.

The solar production profiles in various minerals are shown in figure 2 for $(J_s, R_0) = (100, 100)$ and $(125, 125)$, after the GCR contribution has been added. The total production rates are given in tables 4 and 5 for some selected depths and sizes. In all cases, the ^{22}Ne production rate is higher than that of ^{21}Ne and the $^{22}Ne/^{21}Ne$ ratio monotonically decreases with depth (figure.2), approaching the pure GCR value at about 5 cm. The high ratio in feldspars of ~ 3 is mainly due to ^{23}Na (p, pn) ^{22}Na reaction, which is very favourable.

The above calculations can be compared with the observed values in minerals separated from chondrites. Bochsler *et al* (1969) and Cressy and Bogard (1976) made measurements of neon isotopes in mineral separates from Bruderheim, Elenovka, etc. Their data show that the $^{22}Ne/^{21}Ne$ ratio is directly correlated with Si content and inversely with Mg content. In Bruderheim silicates, where Mg/Si varies between 0·5 and 1·2, the $^{22}Ne/^{21}Ne$ ratio ranges between 1·09 and 1·14. Elenovka feldspars, $^{22}Ne/^{21}Ne = 1{\cdot}25$ for pure Si (Mg/Si = 0). The shielding depths within the meteoroids are however not known. We can obtain some rough estimates of shielding depths from the track density data. Bruderheim was a shower and the fragments, in general, had high ablation, 6–15 cm as estimated in a few cases by Bhandari *et al* (1980). Elenovka was also a multiple fall and the three fragments analysed had shielding depths between 3 and 9 cm (Bhandari *et al* 1980). These observed values can be compared with the calculated ratios given in figures 1 and 2. The calculated $^{22}Ne/^{21}Ne$ ratio (at shielding depth of 3 cm) in olivines and pyroxenes varies between 0·98 and

Table 4. GCR production rates of ^{21}Ne (10^{-8} cc STP/g Ma) in various minerals as a function of depth and radius, R, of the meteoroid.

		Depth (cm)					
Mineral	R (cm)	10	20	30	40	100	At centre
Olivine	9						0·450
	15	0·562					0·562
	25	0·64	0·688				0·688
	50	0·509	0·546	0·513	0·497		0·494
	∞	0·27	0·276	0·237	0·195	0·079	
Feldspar	9						0·211
	15	0·237					0·237
	25	0·247	0·253				0·253
	50	0·195	0·194	0·179	0·172		0·170
	∞	0·1	0·092	0·076	0·06	0·018	
Clinopx	9						0·278
	15	0·336					0·336
	25	0·372	0·392				0·395
	50	0·296	0·310	0·290	0·280		0·278
	∞	0·155	0·158	0·131	0·108	0·04	
Orthopx	9						0·396
	15	0·486					0·486
	25	0·546	0·583				0·583
	50	0·434	0·461	0·432	0·418		0·415
	∞	0·215	0·232	0·197	0·113	0·063	

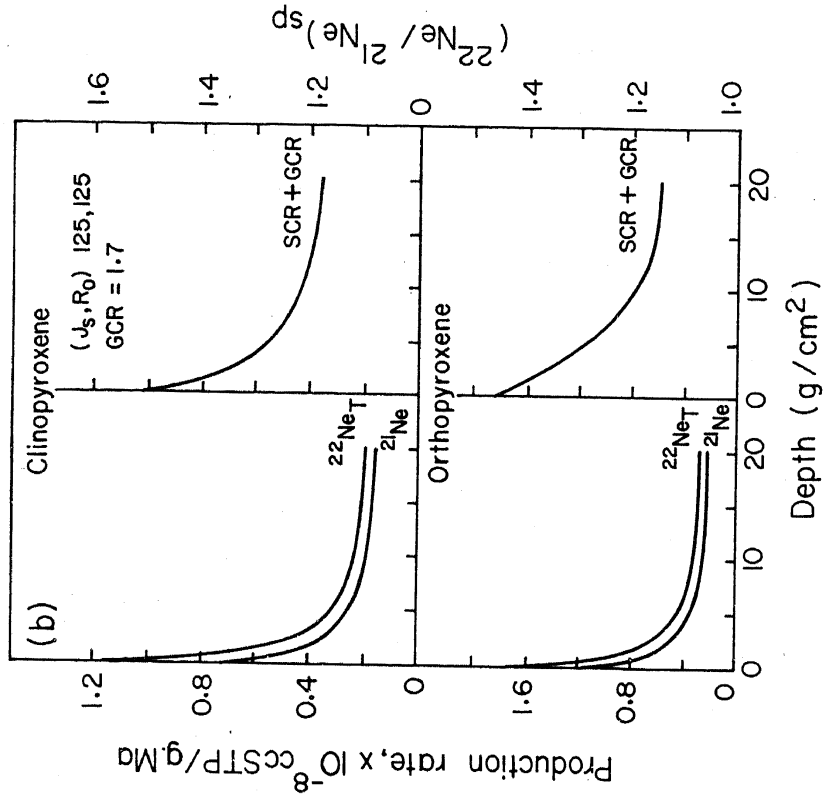
(b)
Clinopyroxene
(J_s, R_o) 125,125
GCR = 1·7
SCR + GCR
$^{22}Ne_T$
^{21}Ne
Orthopyroxene
Production rate, x 10^{-8} ccSTP/g.Ma
Depth (g/cm^2)
$(^{22}Ne/^{21}Ne)_{sp}$

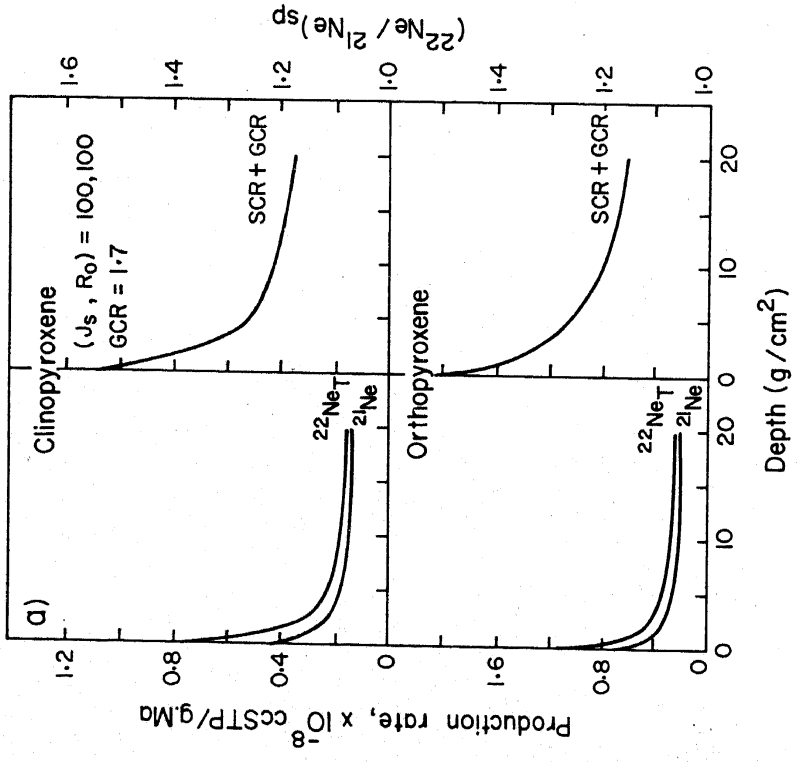
(a)
Clinopyroxene
(J_s, R_o) = 100,100
GCR = 1·7
SCR + GCR
$^{22}Ne_T$
^{21}Ne
Orthopyroxene
Production rate, x 10^{-8} ccSTP/g.Ma
Depth (g/cm^2)
$(^{22}Ne/^{21}Ne)_{sp}$

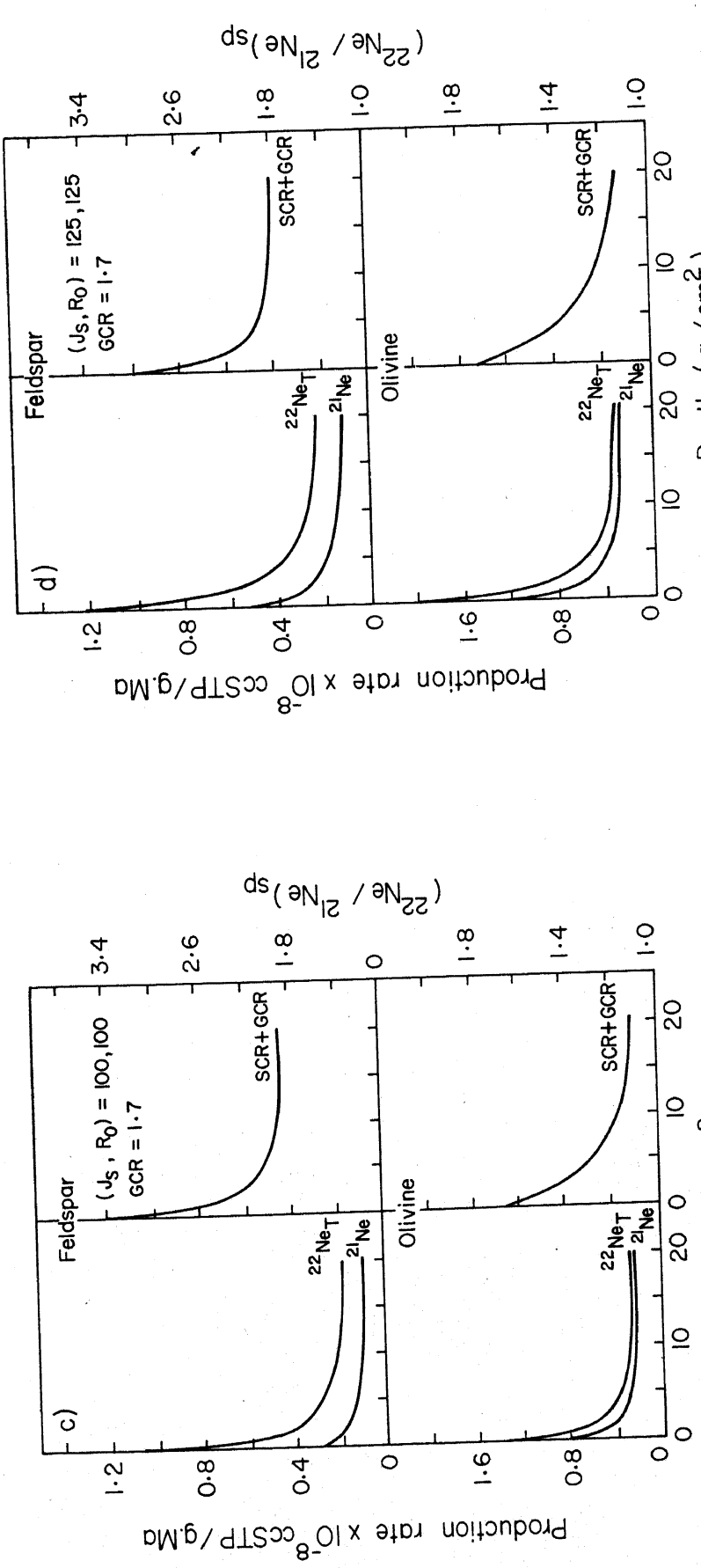

Figure 2. Depth profiles of production rates of ^{21}Ne and ^{22}Ne due to both solar and galactic cosmic rays and $(^{22}Ne/^{21}Ne)_{sp}$ in various minerals located in an infinitely large body. GCR flux of 1·7 P/cm^2 sec. 4π ster and SCR flux parameter values of $(J_s, R_0) = (100,100)$ [in figures (a) and (c)] and (125, 125) [in figures (b) and (d)] have been used.

Table 5. GCR production ratio $^{22}Ne/^{21}Ne$ in various minerals as a function of depth and radius, R, of the meteoroid.

		Depth (cm)					
Mineral	R(cm)	10	20	30	40	100	At centre
Olivine	9						1·122
	15	1·077					1·077
	25	1·042	1·026				1·026
	50	1·041	1·013	1·007	1·003		1·001
	∞	1·055	0·995	0·976	0·974	0·879	
Feldspar	9						1·832
	15	1·947					1·947
	25	2·052	2·109				2·109
	50	2·058	2·158	2·181	2·198		2·205
	∞	2·02	2·21	2·312	2·35	2·925	
Clinopx	9						1·199
	15	1·173					1·173
	25	1·152	1·14				1·141
	50	1·151	1·32	1·128	1·126		1·125
	∞	1·154	1·124	1·107	1·096	1·032	
Orthopx	9						1·149
	15	1·111					1·111
	25	1·082	1·068				1·065
	50	1·081	1·056	1·051	1·047		1·046
	∞	1·087	1·046	1·024	1·014	0·932	

1·18, which is consistent with the values in Bruderheim quoted above. The calculated $^{22}Ne/^{21}Ne$ ratio of 1·15 also compares favourably with the observed value of 1·138 in Elenovka pyroxenes. In the case of feldspars, corrected for their sodium abundance of 4%, we estimate $^{22}Ne/^{21}Ne$ to be 1·5, which is higher than the observed value of 1·25. The reason for this discrepancy may lie in the excitation function for production in sodium. Bochsler *et al* (1969) gave values of $1·07 \pm 0·03$ and $1·35 \pm 0·15$ for $^{22}Ne/^{21}Ne$ for spallation in Mg and Si respectively, which also compare well with the values of 0·96–1·032 and 1·32–1·36 given in table 3 for a 50 cm meteoroid. Thus our calculations seem to give $^{22}Ne/^{21}Ne$ values in silicate minerals in reasonable agreement with the available observations. The ^{21}Ne production rates and $^{22}Ne/^{21}Ne$ profiles are also in agreement with the observations, as shown by the detailed analysis made by Bhandari and Potdar (1982) and Sarafin *et al* (1985) in San Juan Capistrano, Keyes and other meteorites. These profiles can be further refined as better cross-sections and depth profiles in meteorites become available.

Acknowledgements

The author is grateful to Mr K M Suthar for assistance in computations and to Drs P N Shukla, M N Rao and Mr J T Padia for useful comments.

References

Allen R O Jr and Mason B 1973 Minor and trace elements in some meteoritic minerals; *Geochim. Cosmochim. Acta* **37** 1435–1456

Aylmer D, Begemann F, Cloth P, Dragovitsch P, Englert P, Filges D, Herpers U, Herzog G F, Jermaikan A, Klein J, Kruse T H, Michel R, Moniot R K, Middleton R, Peiffer F, Signer P, Stück R, Theis S, Tuniz C, Vadja S, Weber H and Wieler R 1987 Monte Carlo modelling and comparison with experiment of the nuclide production in thick stony targets isotropically irradiated with 600 MeV protons; Report ISSN 0366–0885 Kernfirschungsanlage Julich Gmbh

Baros F and Regnier S 1984 Measurement of cross-sections for ^{22}Na, $^{20-22}$Ne and $^{36-42}$Ar in the spallation of Mg, Al, Si, Ca and Fe. Production ratios of some cosmogenic nuclides in meteorites; *J. Phys.* **45** 855–861

Bhandari N and Potdar M B 1982 Cosmogenic ^{21}Ne and ^{22}Ne depth profiles in chondrites; *Earth Planet. Sci. Lett.* **58** 116–128

Bhandari N, Bhattacharya S K and Padia J T 1975 The surface radioactivity of lunar rocks: implications to solar activity in the past; *Proc. 6th Lunar Sci. Conf. Geochim. Cosmochim. Acta Suppl.* **7** 1913–1925

Bhandari N, Lal D, Rajan R S, Arnold J R, Marti K and Moore C B 1980 Atmospheric ablation in meteorites: a study based on cosmic ray tracks and neon isotopes: *Nucl. Tracks* **4** 213–262

Bhattacharya S K, Imamura M, Sinha N and Bhandari N 1980 Depth and size dependence of ^{53}Mn activity in chondrites; *Earth Planet. Sci. Lett.* **51** 45–57

Bochsler H, Eberhardt P, Geiss J and Grögler N 1969 Rare gas measurements in separate mineral phases of the Otis and Elenovka chondrites. In *Meteorite research* (ed) P M Millman (Dordrecht: D Reidel) pp. 857–874

Cressy P J and Bogard D D 1976 On the calculation of cosmic ray exposure ages of stone meteorites: *Geochim. Cosmochim. Acta.* **40** 749–762

Eberhardt P, Eugster O, Geiss J and Marti K 1966 Rare gas measurements in 30 meteorites; *Z. Naturforsch.* **21** 414–440

Graf Th, Signer P and Wieler R 1986 Production rates of light noble gases, ^{10}Be and ^{26}Al in chondrites; *Meteoritics* **21** 376–377

Kohl C P, Murrel M T, Russ G P III and Arnold J R 1978 Evidence for the constancy of the solar cosmic ray flux over the past ten million years: ^{53}Mn and ^{26}Al measurements; *Proc. 9th Lunar Sci. Conf. Geochim. Cosmochim. Acta Suppl.* **10** 2299–2310

Lal D and Marti K 1977 On the flux of low energy particles in the solar system: The record in St Severin meteorite; *Nucl. Track Detect.* **1** 127–130

Michel R, Dragovitsch P, Englert P, Peiffer F, Stuck R, Theis S, Begemann F, Weder H, Signer P, Wieler R, Filges D and Cloth P 1986 On the depth dependence of spallation reactions in a spherical thick diorite target homogeneously irradiated by 600 MeV protons: *Nucl. Instr. Meth. Phys. Res.* **B16** 61–82

Potdar M B, Bhandari N and Suthar K M 1986 Radionuclide depth profiles in Dhajala chondrite; *Proc. Indian Acad. Sci. (Earth Planet. Sci.)* **95** 169–182

Reedy R C, Herzog G F and Jessberger E K 1979 The reaction Mg (n, α) Ne at 14·1 and 14·7 MeV: Cross-sections and implications for meteorites; *Earth Planet. Sci. Lett.* **44** 341–348

Reedy R C and Arnold J R 1972 Interaction of solar and galactic cosmic ray particles with the moon; *J. Geophys. Res.* **77** 537–555

Sarafin R, Bourot-Denise M, Crozaz G, Herpers U, Pellas P, Schultz L and Weber H W 1985 Cosmic ray effects in the Antarctic meteorite Allan Hills 78084; *Earth Planet. Sci. Lett.* **73** 171–182

Tobailem J 1981 Sections efficaces des reactions nucleaires induites par protons, deutons, particules alpha V-Silicium. Note CEA-N-1466 (5)

Tobailem J and Lassus St Genies C H 1977 Sections efficaces des reactions nucleaires induites par protons, deutons, particules alpha, IV-Aluminium, Note CEA-N-1466 (4)

Walton J R 1974 *Production of He, Ne and Ar in lunar material by solar cosmic ray protons*; PhD thesis, Rice University, USA

Walton J R, Heymann D, Yaniv A, Edgerley D and Rowe M W 1976 Cross-sections for He and Ne isotopes in natural Mg, Al and Si, He isotopes in CaF_2, Ar isotopes in natural Ca and radionuclides in natural Al, Si, Ti, Cr and stainless steel induced by 12 to 45 MeV protons; *J. Geophys. Res.* **81** 5689–5699